Optical gaps of free and embedded Si nanoclusters: Density functional theory calculations

Timothy J. Pennycook,[1,2,*] George Hadjisavvas,[3] Juan C. Idrobo,[1,2] Pantelis C. Kelires,[3] and Sokrates T. Pantelides[1,2]
[1]*Department of Physics & Astronomy, Vanderbilt University, Nashville, Tennessee 37235, USA*
[2]*Materials Science & Technology Division, Oak Ridge National Laboratory, Oak Ridge, Tennessee 37831, USA*
[3]*Department of Mechanical and Materials Science Engineering, Cyprus University of Technology, P.O. Box 50329, 3603 Limassol, Cyprus*

(Received 5 May 2010; revised manuscript received 17 August 2010; published 9 September 2010)

The optical gaps of free and embedded Si nanoclusters are studied within the time-dependent local-density approximation. The effects of deformation, the bonding of individual O atoms on the surface, and coverage by SiO_2 layers on the highest occupied molecular orbital-lowest unoccupied molecular orbital and optical gaps are systematically compared. It is found that all three can have a significant impact. Oxygen bonded to the surface and deformation cause the greatest reduction in the gaps, particularly in combination.

DOI: 10.1103/PhysRevB.82.125310 PACS number(s): 73.22.−f, 71.15.Mb, 78.67.Bf

I. INTRODUCTION

The tunable optical properties of nanoclusters make them attractive candidates for a diverse variety of applications. Among these are lasers, biomarkers, solar cells, displays, and optoelectronics, for which Si nanoclusters (Si-NCs) are of particular interest.[1–6] Simulations show that the optical band gap of perfect isolated Si-NCs increases roughly as the inverse of their diameter from the bulk Si gap of 1.1–5 eV or more.[4,7,8] Real Si-NCs are rarely isolated or perfect, however, and experimental reports of the tunable range of the gap vary significantly. For Si-NCs greater than 3 nm in diameter, the optical gaps generally increase with decreasing diameter as predicted for perfect isolated Si-NCs. Below 3 nm, however, the energy gaps open up much more slowly, reaching only 2–3.5 eV.[9–15] The optical properties of Si-NCs have also been studies over a wider range of energies.[16–18]

Many studies have been devoted to understanding the optical gaps of small Si-NCs. The observation that Si-NCs with photoluminescence (PL) peak energies between 2–3 eV all had PL peaks at ~2 eV after exposure to oxygen[10] led many to believe that O bonds on the surface of the NCs cause the reduced optical gaps. Subsequent theoretical studies[4,10,19–25] showed that O atoms bonded to the surface of ideal Si-NCs indeed introduce localized defect states within the band gaps, reducing or eliminating the opening of the highest occupied molecular orbital-lowest unoccupied molecular orbital (HOMO-LUMO) gaps due to quantum confinement. Other experimental studies have reported little difference in the optical gaps with or without O but the gaps are still considerably smaller than would be expected for a perfect isolated nanocluster.[13,26] More recent theoretical studies have considered nanoclusters that are not isolated but embedded in SiO_2.[5,20,27–34] These studies revealed that the HOMO or LUMO charge densities extend into the oxide overlayer, reducing the confinement and therefore the gaps. Additionally, an effort has recently been made to realistically simulate the deformation of NCs that can occur when they are embedded in an amorphous matrix.[35] Calculations of the densities of states (DOS) reveal that deformation alone can cause significant changes to the band gap.[32]

In this paper we compare the effects of deformation, O impurities, and oxide coverage on the optical gaps of small Si-NCs using real-space linear-response calculations within the time-dependent local-density approximation (TDLDA).[36] The TDLDA approach extends ground-state-density functional theory[37,38] (DFT) to properly and efficiently describe excited states and optical transition probabilities. TDLDA significantly increases the optical gaps of semiconductor and *s*- and *d*-electron metal nanoclusters, bringing them into much better alignment with experimental values than LDA.[19,39] So far TDLDA has been used to study free Si nanoclusters.[19,40] By systematically comparing the photoabsorption for undeformed and deformed 0.75 nm clusters as they are increasingly oxidized we demonstrate that deformation, O impurities and oxide coverage all decrease the size of the optical gaps. Furthermore, by examining the charge densities of the states that are actually involved in the lowest energy optical transitions we show that both localized defect states and reduced quantum confinement due to wavefunction spillage cause reduction in the optical gap. These observations explain the wide variety of experimental results seen for Si-NCs both in porous Si and embedded in SiO_2.

II. COMPUTATIONAL METHODS

The deformed Si-NCs embedded in amorphous SiO_2 were generated as in,[32,35] starting with a supercell of SiO_2 containing 192 atoms in the cubic β-crystobalite structure, which is the closest to the diamond structure among the SiO_2 polymorphs. The supercell is 14.32 Å on each side. The O atoms within a 0.75 nm sphere are removed, leaving behind an embedded 13 atom Si-NC. The structure is then relaxed using DFT before the SiO_2 is amorphized and the Si-NC deformed. The DFT relaxations were performed in the generalized-gradient approximation with a plane-wave basis and projected-augmented wave potentials[41,42] as implemented in the Vienna *ab initio* simulation package (VASP) code.[43–45] The calculations were performed using only the Γ point in *k* space with an energy cutoff of 400 eV. The residual forces on the atoms in the relaxed structure were less than 1 meV/Å.

To amorphize SiO_2 and deform the embedded Si-NCs we used the Monte Carlo algorithm of Wooten *et al.*[46] This method is a well-established means of generating continuous

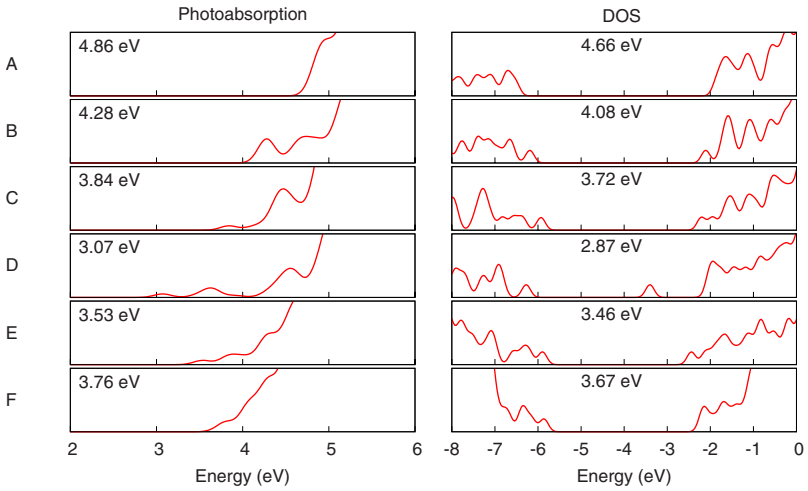

FIG. 1. (Color online) TDLDA photoabsorption and the LDA DOS for the undeformed Si-NCs at various levels of oxidation. A has no O, B has one O bridge bond, C has two O bridge bonds, D has one O double bond, E has one layer of oxide, and F has two layers of oxide. The corresponding TDLDA optical and LDA HOMO-LUMO gaps are indicated.

random networks from perfect crystals using bond breaking and switching moves. A Keating-type valence force model[47,48] is used to approximate the energy of the system. After each attempted move the structure around the bond is relaxed using a steepest-descent method, minimizing the forces on the atoms. The energy of the relaxed structure is then compared to the energy before the attempted move, and the move is accepted or rejected according to the Metropolis criterion. Bond switching moves are periodically followed by volume relaxation to relieve stresses in the system.

Bond switching is first performed in only the oxide at high temperature ($k_BT=3$ eV) for 40 000 moves, allowing it to liquefy. The temperature is subsequently gradually reduced to $k_BT=0.1$ eV over more than 10^6 moves, leaving the oxide in a glassy amorphous state. Additional bond switching is then performed allowing moves in the NC as well as the oxide for 3×10^6 moves. This last step topologically equilibrates the composite system and deforms the Si-NC.

To separate the effects of the oxide matrix and the O bonded to the surface of the NC on the photoabsorption, we produced structures in which we progressively removed layers of the SiO_2, leaving behind the two O atoms bridge bonded to the NC which resulted from the deformation process. We next produced structures in which we stripped off these remaining O atoms one at a time. We also placed a single double bonded O atom on the surface of the stripped cluster to check what effect it would have compared to the bridge bonds. All dangling bonds were passivated with H and the resulting structures relaxed using DFT with VASP. To determine the role of deformation, we also generated a set of undeformed 13 atom Si-NCs with similar types and levels of oxygen and oxide coverage. To generate these structures we started with a supercell of bulk crystalline Si and removed Si atoms such that we were left with a Si-NC of the same size as the deformed clusters. We then added the same types of O bonds as on the surfaces of the deformed NCs and relaxed the structures after passivating the dangling bonds. Undeformed Si-NCs with additional overlayers of SiO_2 were constructed similarly, with the dangling bonds being passivated with additional Si or O atoms and the dangling bonds of the overlayers passivated with H before being relaxed.

Photoabsorption spectra were obtained from each of the structures by placing them in a large spherical domain, outside of which their wave functions were required to vanish. The LDA wave functions were then calculated in real space within the framework of the higher-order finite-difference *ab initio* pseudopotential method,[49] utilizing a Chebyshev-Davidson eigenvalue algorithm.[50] Finally, the optical-absorption spectra were calculated from the LDA wave functions using a linear-response formalism within the TDLDA, as implemented in the PARSEC code,[51,52] in which both the Coulomb and exchange-correlation interactions are taken into account in the electrostatic screening produced by electrons and holes.

Tests were performed to determine the real-space grid spacing required for each of the atomic species in the calculations. For structures containing only Si and H a grid spacing of 0.8 Bohr was used. A grid spacing of 0.5 Bohr was used for calculations containing O atoms. Up to 400 energy levels were used to compute the LDA wave functions, which were required to vanish at a radius of 35 Bohr. In the calculation of the TDLDA photoabsorption itself, the number of bands included was increased until the photoabsorption was converged up to 6 eV, to allow reliable comparisons of the optical gaps.

III. RESULTS AND DISCUSSION

The TDLDA photoabsorption spectra are shown alongside the LDA DOS for the undeformed NCs in Fig. 1 and for the deformed NCs in Fig. 2. The photoabsorption spectra and DOS have been broadened by a Gaussian with a 0.1 eV full-width-half-maximum, normalized by the total number of electrons and displayed on the same scale. We define the optical gap as the energy at which the oscillator strength reaches 0.1% of the oscillator strength integrated from 0 to 5 eV. The optical gaps and LDA HOMO-LUMO gaps are indicated in Figs. 1 and 2.

The optical gap of the bare undeformed NC is 4.86 eV, slightly larger than the 4.66 eV LDA band gap. Adding first one then two O bridge bonds to the surface of the cluster reduces the optical gap to 4.28 eV and 3.84 eV, respectively. The DOS for the bridge-bonded clusters resemble that of the bare cluster but with extra peaks just above the LUMO and below the HOMO of the bare cluster. The extra peaks reduce

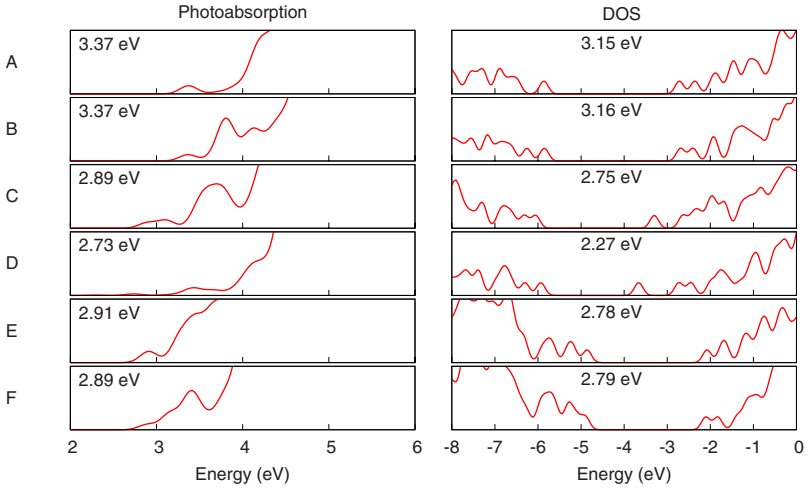

FIG. 2. (Color online) TDLDA photoabsorption and the LDA DOS for the deformed Si-NCs at various levels of oxidation. A has no O, B has one O bridge bond, C has two O bridge bonds, D has one O double bond, E has one layer of oxide, and F has two layers of oxide. The corresponding TDLDA optical and LDA HOMO-LUMO gaps are indicated.

the size of the band gap allowing optical transitions to occur at lower energies than in the bare cluster.

Replacing the bridge bonded O atoms with a single double bonded O atom also introduces DOS peaks inside the band gap. Although the HOMO is at about the same energy as the HOMO of the cluster with a single bridge-bonded O atom, the LUMO is much deeper inside the gap. The first unfilled state appears 1.37 eV below the next lowest state in the DOS. The optical gap of the double bonded cluster is correspondingly smaller, with a size of 3.07 eV.

We next add a layer of O atoms around the cluster with two bridge bonds. O atoms now passivate the Si atoms and H atoms passivate the O atoms in the overlayer. Adding the O layer reduces the HOMO-LUMO gap by 0.26 eV. The optical gap similarly decreases by 0.21 eV. Adding a layer of Si atoms over the O layer, making a layer of SiO_2, increases the HOMO-LUMO gap to 3.67 eV, only 0.05 eV lower than the cluster with just two bridge-bonded O atoms. The optical gap increases up to 3.76 eV, also only slightly lower than for the cluster with only the two bridge-bonded O atoms.

Turning now to the realistically deformed NCs, we find that deformation alone greatly reduces the optical gap. The bare deformed cluster has a HOMO-LUMO gap of 3.15 eV and an optical gap of 3.37 eV, both 1.49 eV lower than that of the bare undeformed cluster. The only undeformed cluster with smaller gaps is the one with an O double bond, the rest all have larger optical and HOMO-LUMO gaps. Adding a single O bridge-bond makes no significant difference to the gaps, as might be expected from the fact that the deformation reduces the gap more than the double-bond on the undeformed cluster. The DOS of the deformed cluster with and without a single bridge-bond look fairly similar but the bridge bond adds a second peak below the energy of the HOMO. Correspondingly, a peak appears in the photoabsorption around 3.8 eV which is not there without the bridge-bond.

Adding a second bridge-bond, moves the HOMO peak slightly down in energy but also introduces a peak in the unoccupied DOS significantly lower in energy than the LUMO of the bare cluster. The optical gap is correspondingly reduced by 0.48–2.89 eV. Replacing the bridge bonds with a single double bond produces similar HOMO and HOMO-1 peaks but moves the LUMO DOS peak even lower in energy, resulting in a 2.73 eV optical gap. We note that the TDLDA spectrum presents an optical excitation at ~2.3 eV with a nonzero oscillator strength, however, its magnitude is small compared to the other optical transitions shown in Fig. 2, D. As its optical strength is nonzero it is not a forbidden transition. Finally, as with the undeformed cluster, covering the deformed cluster with two bridge bonds with SiO_2 matrix does not significantly alter the optical gap, suggesting that those O atoms bonded to the surface of NCs have the most influence on the size of the band gap.

In order to further investigate the nature of the states that reduce the size of the optical gaps, we have plotted isosurfaces of the charge densities of the states which are actually participating in the lowest TDLDA photoabsorption transitions. From Fig. 3 it can be seen that the states introduced into the HOMO-LUMO gap of the bare clusters by single O atom double bonds are concentrated around the O atom. Re-

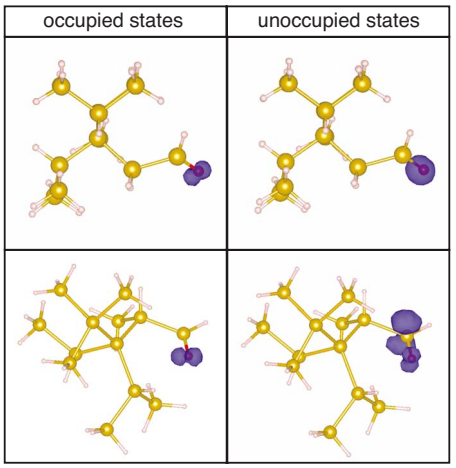

FIG. 3. (Color online) Charge density isosurfaces (dark blue) superimposed on the structures of the undeformed (top) and deformed (bottom) Si-NCs with a single O atom (dark/red) double bonded to their surfaces. Si atoms are shown as large gold balls and H as small light pink colored balls. The charge densities are weighted according to each state's contribution to the TDLDA photoabsorption strength up to 4 eV for the undeformed structure and 3 eV for the deformed structure. Isosurfaces are plotted at 10% of the maximum charge density.

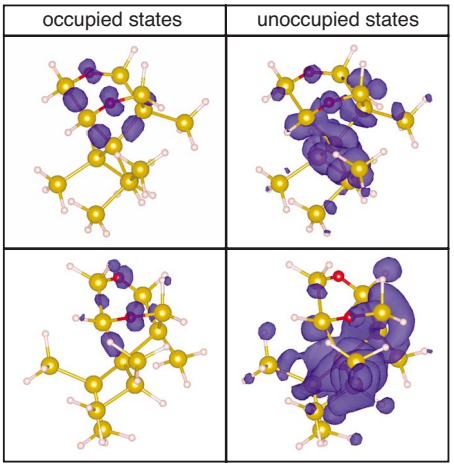

FIG. 4. (Color online) Charge density isosurfaces (dark blue) superimposed on the structures of the undeformed (top) and deformed (bottom) Si-NCs with two O (dark/red) atoms bridge bonded to their surfaces. Si atoms are shown as large gold balls and H as small light pink colored balls. The charge densities are weighted according to each state's contribution to the TDLDA photoabsorption strength up to 5 eV for the undeformed structure and 4 eV for the deformed structure. Isosurfaces are plotted at 10% of the maximum charge density.

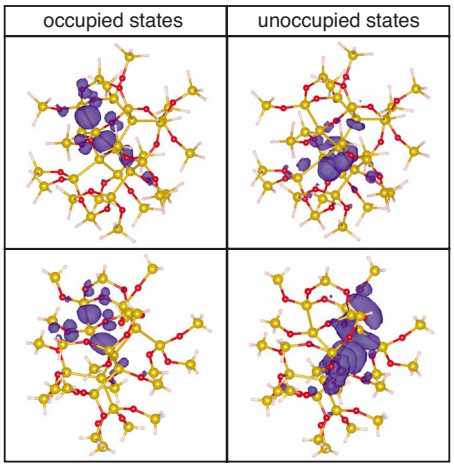

FIG. 5. (Color online) Charge density isosurfaces (dark blue) superimposed on the structures of the undeformed (top) and deformed (bottom) Si-NCs with two O atoms bridge bonded to their surfaces and covered in a full layer of SiO_2. Si atoms are shown as large gold balls, O as smaller red balls and H as small light pink colored balls. The charge densities are weighted according to each state's contribution to the TDLDA photoabsorption strength up to 4 eV for the undeformed structure and 3 eV for the deformed structure. Isosurfaces are plotted at 10% of the maximum charge density.

ducing the isosurface level, however, we find that these states also extend to other parts of the nanocluster, which explains why the deformation of the nanocluster would affect the energies of these defect states. The bridge bonds shown in Fig. 4 also introduce optical gap-reducing states which are concentrated around the O atoms. The charge density of these gap-reducing states is less localized than those introduced by the double bonds and this maybe the reason the optical gaps of the NCs with bridge bonds are more sensitive to deformation than those with double bonded O atoms. Finally, one can see from Fig. 5 that adding a layer of SiO_2 over the NCs with bridge bonded O atoms makes only minor differences to the spatial localization of the states which limit the size of the optical gaps. The charge density leaks out into the oxide somewhat, explaining the slightly lower optical gaps but is mostly concentrated in the same areas of the NCs as without the oxide.

The present results are in agreement with previous theoretical work showing that the optical gaps of small Si-NCs are reduced by the presence of O bonded to their surfaces.[4,10,19–24] Previous theoretical studies of embedded Si-NCs agree that the matrix reduces the HOMO-LUMO gaps but a number of different conclusions are reached. Some conclude that the gap shrinkage is mainly due to reduced quantum confinement due to the wave functions leaking out into the matrix.[5,27–29,31] Others show that similar gaps are produced before and after most of the embedding SiO_2 have been removed, leaving behind only O atoms bonded to the surface of the NCs, indicating the importance of O bonds on the surface of the Si-NCs.[33,34] Some studies also point out that the interface between Si-NC and bulk SiO_2 matrix is not likely to be abrupt and that strain and deformation can reduce the gaps.[20,30,32–34] The present results, the first produced with TDLDA for embedded clusters, show that deformation and localized O impurity states have the greatest impact on the size of the optical gaps of embedded Si-NCs, with reduced confinement due to wave-function spillage causing only relatively minor additional closing. Additionally, although deformation and O bonds on the surfaces of the NCs independently affect the optical gaps, the smallest gaps are caused by a combination of the two.

IV. CONCLUSIONS

From the present calculations it is seen that O bonds and deformation can independently reduce the sizes of the optical gaps of Si-NCs. Additionally, different types of O bonds introduce defect states at different energies and result in different optical gaps. It is clear, however, that when both O and deformation are present, it is not a simple question as to which independently produces the smaller HOMO-LUMO gap. O bonded to the surface of the NCs introduces defect states at different energies depending on whether the NC is deformed or not. The optical gaps of the deformed clusters are smaller than those of the undeformed clusters by 0.34 eV with a double bonded O atom and by 0.95 eV with two bridge-bonded O atoms. In general, it seems that the smallest optical gaps are produced with a combination of deformation and O atoms bonded to the surface of the NCs. In particular, the lowest energy optical gap of 2.73 eV is produced by the combination of deformation and an O double bond. Experimental samples of embedded Si-NCs generally contain NCs with a range of both deformation and O bonds. Macroscale properties such as absorption and photoluminescence depend on the average characteristics. Generally, the largest, most deformed and oxygenated clusters will limit the optical gap with the statistical distribution of the size, deformation and

oxidation determining the shape and width of the optical spectral features. An ideal sample would have a distribution of NCs with size, deformation and oxidation that was tailored to a particular application. For instance, a narrow photoluminescence peak could be achieved at a high energy by using free ultrasmall NCs with the same size, negligible deformation, and no O bonded to their surface. A broad peak could be achieved using NCs of various sizes levels of deformation and O bonding. Achieving the former presents a difficult challenge whereas the latter is what is generally produced.

ACKNOWLEDGMENTS

This work was supported in part by the National Science Foundation GOALI under Grant No. DMR-0513048, by Alcoa, Inc., by the McMinn Endowment at Vanderbilt University, and by the Division of Materials Sciences and Engineering, U.S. Department of Energy. Computations were performed at the National Energy Research Scientific Computing Center, which is supported by the Office of Science of the U.S. Department of Energy under Contract No. DE-AC02-05CH11231.

*t.pennycook@vanderbilt.edu

[1] K. Hirschman, L. Tsybeskov, S. Duttagupta, and P. Fauchet, Nature (London) **384**, 338 (1996).
[2] R. Collins, P. Fauchet, and M. Tischler, Phys. Today **50**, 24 (1997).
[3] A. Fowler, Phys. Today **50**, 50 (1997).
[4] A. Puzder, A. Williamson, J. Grossman, and G. Galli, Phys. Rev. Lett. **88**, 097401 (2002).
[5] K. Seino, F. Bechstedt, and P. Kroll, Nanotechnology **20**, 135702 (2009).
[6] M. Cazzanelli, D. Kovalev, L. Dal Negro, Z. Gaburro, and L. Pavesi, Phys. Rev. Lett. **93**, 207402 (2004).
[7] J. Proot, C. Delerue, and G. Allan, Appl. Phys. Lett. **61**, 1948 (1992).
[8] L. Wang and A. Zunger, J. Phys. Chem. **98**, 2158 (1994).
[9] S. Schuppler, S. L. Friedman, M. A. Marcus, D. L. Adler, Y. H. Xie, F. M. Ross, Y. J. Chabal, T. D. Harris, L. E. Brus, W. L. Brown, E. E. Chaban, P. F. Szajowski, S. B. Christman, and P. H. Citrin, Phys. Rev. B **52**, 4910 (1995).
[10] M. V. Wolkin, J. Jorne, P. M. Fauchet, G. Allan, and C. Delerue, Phys. Rev. Lett. **82**, 197 (1999).
[11] D. Kovalev, E. Gross, N. Künzner, F. Koch, V. Y. Timoshenko, and M. Fujii, Phys. Rev. Lett. **89**, 137401 (2002).
[12] M. Carrada, A. Wellner, V. Paillard, C. Bonafos, H. Coffin, and A. Claverie, Appl. Phys. Lett. **87**, 251911 (2005).
[13] T. van Buuren, L. N. Dinh, L. L. Chase, W. J. Siekhaus, and L. J. Terminello, Phys. Rev. Lett. **80**, 3803 (1998).
[14] J. von Behren, T. van Buuren, M. Zacharias, E. H. Chimowitz, and P. M. Fauchet, Solid State Commun. **105**, 317 (1998).
[15] L. Patrone, D. Nelson, V. Safarov, M. Sentis, W. Marine, and S. Giorgio, J. Appl. Phys. **87**, 3829 (2000).
[16] K. D. Rinnen and M. L. Mandich, Phys. Rev. Lett. **69**, 1823 (1992).
[17] J. C. Idrobo, M. Yang, K. A. Jackson, and S. Öğüt, Phys. Rev. B **74**, 153410 (2006).
[18] J. C. Idrobo, A. Halabica, R. H. Magruder III, R. F. Haglund, Jr., S. J. Pennycook, and S. T. Pantelides, Phys. Rev. B **79**, 125322 (2009).
[19] I. Vasiliev, J. R. Chelikowsky, and R. M. Martin, Phys. Rev. B **65**, 121302 (2002).
[20] M. Luppi and S. Ossicini, Phys. Rev. B **71**, 035340 (2005).
[21] Z. Zhou, L. Brus, and R. Friesner, Nano Lett. **3**, 163 (2003).
[22] A. Puzder, A. Williamson, J. Grossman, and G. Galli, J. Am. Chem. Soc. **125**, 2786 (2003).
[23] E. Luppi, E. Degoli, G. Cantele, S. Ossicini, R. Magri, D. Ninno, O. Bisi, O. Pulci, G. Onida, M. Gatti, A. Incze, and R. D. Sole, Opt. Mater. **27**, 1008 (2005).
[24] Q. S. Li, R. Q. Zhang, S. T. Lee, T. A. Niehaus, and T. Frauenheim, Appl. Phys. Lett. **91**, 043106 (2007).
[25] C. S. Garoufalis and A. D. Zdetsis, Phys. Chem. Chem. Phys. **8**, 808 (2006).
[26] A. Seraphin, S. Ngiam, and K. Kolenbrander, J. Appl. Phys. **80**, 6429 (1996).
[27] L. E. Ramos, J. Furthmüller, and F. Bechstedt, Appl. Phys. Lett. **87**, 143113 (2005).
[28] L. E. Ramos, J. Furthmüller, and F. Bechstedt, Phys. Rev. B **70**, 033311 (2004).
[29] L. E. Ramos, J. Furthmüller, and F. Bechstedt, Phys. Rev. B **71**, 035328 (2005).
[30] N. Daldosso, M. Luppi, S. Ossicini, E. Degoli, R. Magri, G. Dalba, P. Fornasini, R. Grisenti, F. Rocca, L. Pavesi, S. Boninelli, F. Priolo, C. Spinella, and F. Iacona, Phys. Rev. B **68**, 085327 (2003).
[31] P. Kroll and H. J. Schulte, Phys. Status Solidi B **243**, R47 (2006).
[32] G. Hadjisavvas and P. C. Kelires, Physica E **38**, 99 (2007).
[33] R. Guerra, I. Marri, R. Magri, L. Martin-Samos, O. Pulci, and S. Ossicini, Superlattices Microstruct. **46**, 246 (2009).
[34] R. Guerra, E. Degoli, and S. Ossicini, Phys. Rev. B **80**, 155332 (2009).
[35] G. Hadjisavvas and P. C. Kelires, Phys. Rev. Lett. **93**, 226104 (2004).
[36] S. Öğüt, J. R. Chelikowsky, and S. G. Louie, Phys. Rev. Lett. **79**, 1770 (1997).
[37] P. Hohenberg and W. Kohn, Phys. Rev. **136**, B864 (1964).
[38] W. Kohn and L. J. Sham, Phys. Rev. **140**, A1133 (1965).
[39] M. L. Tiago, J. C. Idrobo, S. Öğüt, J. J. Jellinek, and J. R. Chelikowsky, Phys. Rev. B **79**, 155419 (2009).
[40] M. Lopez del Puerto, M. Jain, and J. R. Chelikowsky, Phys. Rev. B **81**, 035309 (2010).
[41] P. E. Blöchl, Phys. Rev. B **50**, 17953 (1994).
[42] G. Kresse and D. Joubert, Phys. Rev. B **59**, 1758 (1999).
[43] G. Kresse and J. Hafner, Phys. Rev. B **47**, 558 (1993).
[44] G. Kresse and J. Furthmuller, Comput. Mater. Sci. **6**, 15 (1996).
[45] G. Kresse and J. Furthmuller, Phys. Rev. B **54**, 11169 (1996).
[46] F. Wooten, K. Winer, and D. Weaire, Phys. Rev. Lett. **54**, 1392 (1985).
[47] Y. Tu and J. Tersoff, Phys. Rev. Lett. **84**, 4393 (2000).

[48] Y. Tu and J. Tersoff, Phys. Rev. Lett. **89**, 086102 (2002).
[49] J. R. Chelikowsky, N. Troullier, and Y. Saad, Phys. Rev. Lett. **72**, 1240 (1994).
[50] Y. Zhou, Y. Saad, M. L. Tiago, and J. R. Chelikowsky, Phys. Rev. E **74**, 066704 (2006).
[51] M. E. Casida, in *Recent Advances in Density-Functional Methods, Part I*, edited by D. P. Chong (World Scientific, Singapore, 1995), p. 155; *Recent Developments and Applications of Modern Density Functional Theory*, edited by J. M. Seminario (Elsevier, Amsterdam, 1996), p. 391.
[52] I. Vasiliev, S. Öğüt, and J. R. Chelikowsky, Phys. Rev. B **65**, 115416 (2002).